

Bismuth sodium titanate based lead-free ceramic/epoxy 1–3 composites: fabrication and electromechanical properties

Feng Li & Ruzhong Zuo

**Journal of Materials Science:
Materials in Electronics**

ISSN 0957-4522
Volume 25
Number 6

J Mater Sci: Mater Electron (2014)
25:2730–2736
DOI 10.1007/s10854-014-1936-9



Your article is protected by copyright and all rights are held exclusively by Springer Science +Business Media New York. This e-offprint is for personal use only and shall not be self-archived in electronic repositories. If you wish to self-archive your article, please use the accepted manuscript version for posting on your own website. You may further deposit the accepted manuscript version in any repository, provided it is only made publicly available 12 months after official publication or later and provided acknowledgement is given to the original source of publication and a link is inserted to the published article on Springer's website. The link must be accompanied by the following text: "The final publication is available at link.springer.com".

Bismuth sodium titanate based lead-free ceramic/epoxy 1–3 composites: fabrication and electromechanical properties

Feng Li · Ruzhong Zuo

Received: 7 February 2014 / Accepted: 7 April 2014 / Published online: 17 April 2014
© Springer Science+Business Media New York 2014

Abstract The 1–3 piezocomposites based on $0.96\text{Bi}_{0.5}(\text{Na}_{0.84}\text{K}_{0.16})_{0.5}\text{TiO}_3-0.04\text{SrTiO}_3$ (BNKT–ST) were fabricated by a modified dice-fill method. Electro-mechanical properties of the composites as a function of the ceramic volume fraction (ν) were measured and compared with theoretical values as well as with those of monolithic ceramics. The as-prepared piezocomposite with $\nu = 0.276$ showed a clear single thickness mode with a relatively high resonance frequency of more than 2 MHz, together with a relatively high piezoelectric strain constant ($d_{33} \sim 104$ pC/N), a high thickness coupling coefficient ($k_t \sim 0.547$), low acoustic impedance ($Z \sim 9$ Mrayls) and a large piezoelectric voltage coefficient ($g_{33} \sim 91.5 \times 10^{-3} \text{ m}^2/\text{C}$). From the practical application point of view, these promising results indicate that the BNKT–ST ceramic/epoxy 1–3 composite has great potential to be used in biomedical ultrasonic transducers as well as nondestructive evaluations.

1 Introduction

It is well known that the ubiquitous lead zirconium titanate (PZT) based piezoelectric ceramics have been the mainstay for sensors, actuators, transducers in electronic devices because of their superior performances [1, 2]. However, due to the high lead vaporization and contamination during the processing and disposal, which triggers a crucial environment pollution problem, the extensive use of PZT-

based piezoelectric ceramics and related composites have been tremendously restricted regardless of their superior performances [3–6]. Hence these mentioned problems make the replacement of PZT-based ceramics/composites imperative.

Following these tendencies, lead-free piezoelectric ceramic became a hot topic to researchers in recent decades [7, 8]. Bismuth sodium titanate ($\text{Bi}_{1/2}\text{Na}_{1/2}\text{TiO}_3$) (BNT) composition was one type of the most important lead-free ceramics with a perovskite structure discovered by Smolenskii et al. [9–11]. Previous reports of the BNT-based ceramics indicated that they were promising lead-free materials for ultrasonic transducer applications since BNT-based ceramics showed good performances and conformed to the requirements of biomedical ultrasonic transducers to some degree [12–15].

Unfortunately, two intrinsic drawbacks for monolithic ceramic materials still exist. One is the high acoustic impedance (~ 30 Mrayls), resulting in the acoustic impedance mismatch with human tissues or water (~ 1.5 Mrayls), and the other is that those hybrid resonance modes exert a harmful effect on the thickness resonance mode, both of which would result in fuzzy ultrasonic imaging inevitably in the medical ultrasonic applications. In order to overcome these bottlenecks, the piezoceramics are often incorporated into passive polymer to form 1–3 composites. The so called 1–3 composite, which consists of a parallel array of ceramic rods in the passive polymer matrix, could effectively improve the electromechanical coupling coefficient in the thickness mode and rapidly cut down acoustic impedance value [16–18]. Moreover, an early survey of the suitability of the various composite structures for pulse-echo ultrasonic applications identified the 1–3 composites geometry as the most promising one [19]. Therefore, the ceramic/polymer piezocomposite with

F. Li · R. Zuo (✉)
Institute of Electro Ceramics and Devices, School of Materials
Science and Engineering, Hefei University of Technology,
Hefei 230009, People's Republic of China
e-mail: piezolab@hfut.edu.cn

1–3 connectivity have become an important material in the design and manufacture of thickness mode transducers for biomedical ultrasonic imaging. The major reasons are that, compared to monolithic piezoelectric ceramics, 1–3 piezocomposite can be designed with higher thickness coupling coefficient, lower acoustic impedance and weaker hybrid resonance mode. Moreover, the characteristics of 1–3 composites can be adjusted by easily tailoring the ceramic volume fraction to meet the specific requirements of various applications.

In this study, BNT-based lead-free ceramic/epoxy 1–3 composites were fabricated by a modified dice-fill method [5] owing to its simplicity and high efficiency [6]. The performances of 1–3 composite as a function of the volume fraction of the ceramic phase were shown to have a good agreement with theoretical predictions. Although BNT-based ceramic/epoxy composites have been reported previously, many authors mainly paid much attention to the variation tendencies of the performance parameters in the whole ceramic content range, and rarely focused on the relation between the ceramic content and the requirement of the biomedical transducers [20–25]. However, the 1–3 composite with high ceramic content may not be suitable for the application of the biomedical transducers because of the high acoustic impedance and dielectric permittivity. That is to say, the high acoustic impedance will lead to the mismatch between the transducers probe and the body tissue, the high dielectric permittivity will lead to the electrical impedance mismatching between the transducer and the system instrumentation. In consequence, the detailed investigation of properties for 1–3 composite with relatively low ceramic volume is of great importance but has been ignored so far. The purpose of this work was to identify how the electrical properties changed with ν and then to achieve an overall electromechanical performance, showing advantages to others in transducer applications. Particular attention was paid to the 1–3 piezocomposite with a relatively low ceramic content.

2 Experimental

$0.96\text{Bi}_{0.5}(\text{Na}_{0.84}\text{K}_{0.16})_{0.5}\text{TiO}_3-0.04\text{SrTiO}_3$ (BNKT–ST) ceramic was synthesized by a conventional solid-state reaction method using high-purity (>99 %) Bi_2O_3 , Na_2CO_3 , K_2CO_3 , TiO_2 , SrCO_3 as raw materials. After mixing the oxides and carbonates, then calcined twice at 850 °C for 2 h. BNKT–ST ceramic discs of 15 mm in diameter were prepared by dry pressing and sintered at 1,170 °C for 2 h in air, as described elsewhere [26]. The BNKT–ST/epoxy 1–3 type composites were fabricated by a two-step method in order to eliminate cracks as well as to guarantee final products with a high aspect ratio. A blade of 100 μm

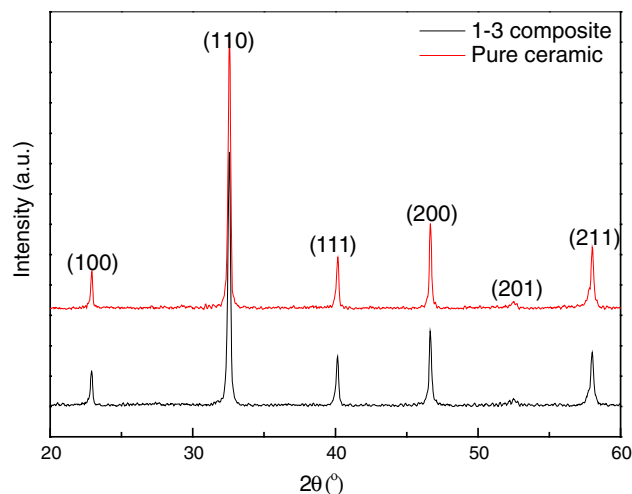


Fig. 1 The XRD pattern of sintered BNKT–ST ceramic and related composite specimen in the 2θ range 20° – 60°

in thickness was used to dice ceramic discs and the width of pillars was varied to tailor the ceramic volume fraction of the composite. A set of parallel grooves were obtained and then filled with epoxy (Resin E51 and Harder 593# in a weight ratio of 1:0.25). After the ceramic pellets were cleaned, the epoxy was poured into the grooves and then degassed in vacuum for 30 min, and the epoxy was cured at 40 °C for 24 h, then a second set of cuts perpendicular to the first ones were made. After filling with epoxy, the composite was dried under the same condition mentioned above. Excess epoxy and ceramics were polished away until the end of ceramic rods appeared, as shown in Fig. 2a. Two parallel major surfaces were deposited with air-dried silver paint for electrical characterizations. The composite samples were poled at 80 °C for 30 min under an electric field of 4.5 kV/mm in a silicone oil bath.

The sample density was measured based on the Archimedes method. The morphology of 1–3 composite samples were observed by scanning electron microscopy (SEM, JEOL JSM-6490LV, Tokyo, Japan). The average piezoelectric constant d_{33} was measured on about 30 dots by a quasi-static Belincourt-meter (YE2730A, Sinocera, Yangzhou, China). The dielectric properties and resonant characteristics were measured by an impedance/gain-phase analyzer (HP4194A). The thickness electromechanical coupling coefficient k_t and acoustic impedance Z were determined by a resonance and anti-resonance method performed on the basis of IEEE standards.

3 Results and discussion

The XRD patterns of sintered BNKT–ST ceramic and related composite specimen in the 2θ range 20° – 60° are

shown in Fig. 1. The single peak of the (111) and (200) planes and material phase at room temperature should be pseudocubic rather than cubic together with the macroscopic properties reported in this system. Another phenomenon should be noted that the diffraction peak location and intensity do not change significantly, which may be due to the fact that dicing process doesn't involve any changes of crystal structure of the ceramic and it is just a macroscopic physical dicing process.

Figure 2 shows the morphology of the BNKT-ST ceramic/epoxy 1–3 composite. As shown in Fig. 2a, b, it can be seen that a defect-free ceramic rod array was well diced and exhibit a periodically ordered structure. Figure 2c displays the cross-section SEM image of 1–3 composite, indicating that the epoxy is well backfilled into the grooves. In addition, as shown in magnified images of Fig. 2d, no visible gaps or physical flaws between the interfaces of the epoxy and ceramic rods can be found, which further illustrates that the epoxy and the ceramic rod have been well bonded based on an appropriate solidifying process. However, some imperfect rectangular ceramic pillars can be seen, which probably due to the inevitable vibration of blades in operation under experimental conditions.

According to the modified series and parallel model presented by Chan and Unsworth [27], the theoretical performance of the composites can be calculated as a

function of the ceramic volume fraction v . The dielectric permittivity ϵ_r , piezoelectric strain constant d_{33} , piezoelectric voltage coefficient g_{33} , electromechanical coupling coefficient k_t and acoustic impedance Z can be calculated using the following equations:

$$\epsilon_{33}^T = v\epsilon_{33, BNKT-ST}^T - v(1-v)(d_{33, BNKT-ST}^c)^2 / s(v) + (1-v)\epsilon_{11, epoxy}^p \tag{1}$$

$$d_{33} = v s_{11, epoxy}^p d_{33, BNKT-ST}^c / s(v) \tag{2}$$

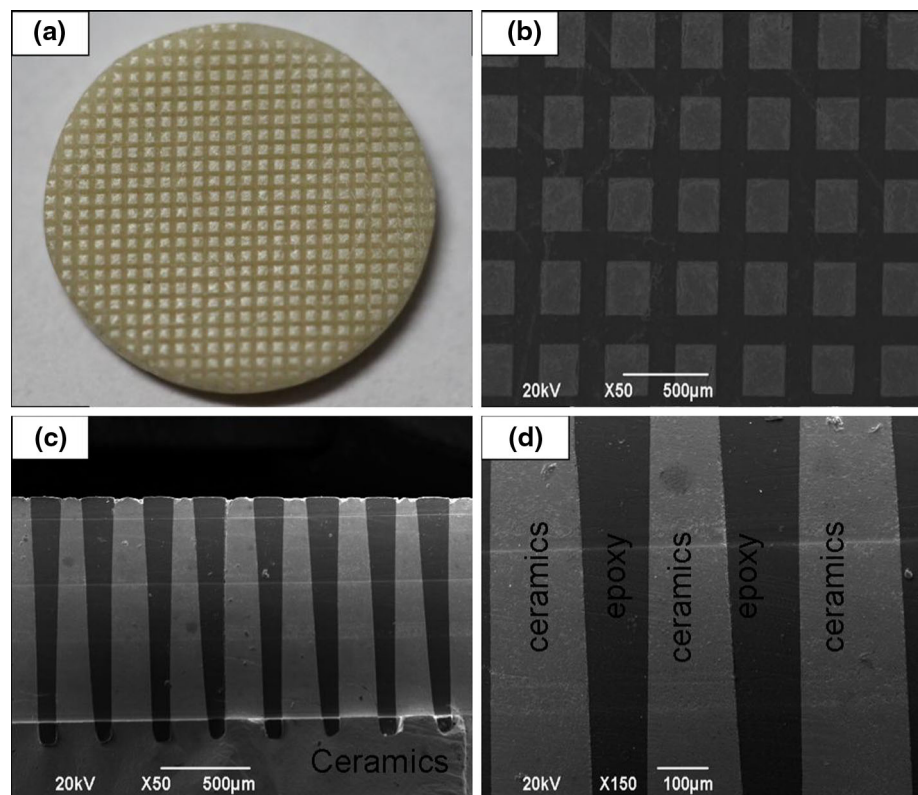
$$g_{33} = d_{33} / \epsilon_{33}^T \tag{3}$$

$$Z = \sqrt{\rho C_{33}^D} \tag{4}$$

$$k_t = \sqrt{1 - C_{33}^E / C_{33}^D} \tag{5}$$

where $s(v) = v s_{11, epoxy}^p + (1-v) s_{33, BNKT-ST}^c$, s is the elastic compliance, C is elastic stiffness, ρ is the density of the composite and ϵ_0 is the permittivity in free space ($=8.85 \times 10^{-12}$ F/m). In Eqs. (1) and (2), v refers to the volume fraction of the bulk ceramic and thus $(1-v)$ is the volume fraction of epoxy in the composite. ϵ_{33}^T is the free dielectric constant in Eqs. (1) and (3). C_{33}^E and C_{33}^D is the elastic stiffness coefficient in Eqs. (4) and (5). The k_t value of the bulk ceramic and the composite was calculated using Eq. (6). The acoustic impedance Z and longitudinal electromechanical coupling coefficient k_{33} of the bulk ceramic

Fig. 2 **a** Photograph of BNKT-ST/epoxy 1–3 composite; **b** the SEM images of the end face of 1–3 composite; **c, d** the cross-section and magnified images of obtained 1–3 composites



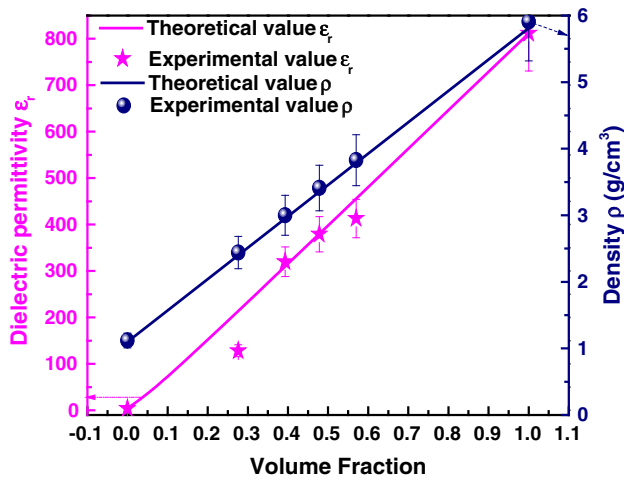


Fig. 3 Comparison between theoretical and experimental values of the density and dielectric permittivity of the BNKT–ST ceramic/epoxy 1–3 composites as a function of the ceramic volume fraction

were determined by a resonance and anti-resonance method, which can be expressed as Eqs. (7), (8) and (9).

$$k_t^2 = \frac{\pi f_s}{2f_p} \tan \frac{\pi(f_p - f_s)}{2f_p} \tag{6}$$

$$Z = \rho V^D \tag{7}$$

$$V^D = 2f_p t \tag{8}$$

and

$$k_{33}^2 = k_p^2 + k_t^2 - k_p^2 \times k_t^2 \tag{9}$$

where t is the thickness of composite, V^D is the spread speed of sound, f_s is resonance frequency and f_p is the antiresonance frequency in the thickness mode.

Figure 3 shows the density ρ and dielectric permittivity ϵ_r at 1 kHz of 1–3 composite as a function of v . It can be seen that the densities of the 1–3 composite linearly increase with increasing the ceramic volume fraction and show a good agreement with theoretical values. According to the Eq. (1), because the dielectric permittivity ϵ_r of monolithic piezoelectric ceramics is far more than that of epoxy, the dielectric permittivity of 1–3 composite exhibits an almost linear relationship with the ceramic volume fraction, although experimental values have some discrepancies compared with the theoretical values. A relatively large discrepancy for the composite with $v = 0.276$ may be ascribed to the difficulty in polling for the composites with low ceramic volume fractions [28]. Fortunately, the depressed dielectric permittivity could be expected to enhance the g_{33} value. On the whole, by using lead-free BNKT–ST ceramic pillars embedded in the epoxy, the 1–3 composite could achieve moderate ϵ_r (100–400) value. According to Zhen et al. [5], a relative

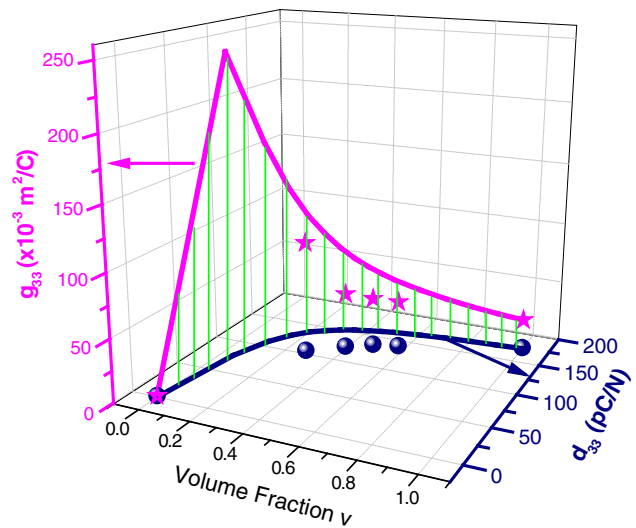


Fig. 4 Comparison between theoretical and experimental values of the piezoelectric strain and voltage coefficients of the BNKT–ST ceramic/epoxy 1–3 composites as a function of the ceramic volume fraction

permittivity in the vicinity of 100 provides a large voltage coefficient and eases the electrical impedance matching between the transducer and the system instrumentation. Hence, the developed 1–3 composites could be suitable to design drive/receive type transducers.

Figure 4 depicts the piezoelectric strain coefficient d_{33} and piezoelectric voltage coefficient g_{33} of the BNKT–ST/epoxy 1–3 composites as a function of the ceramic volume fraction. At the same time, the d_{33} – g_{33} relation can be also obtained from the Fig. 4. It can be seen that the d_{33} value of the composite increases rapidly as $v < 0.3$, then increases mildly at a higher level of the ceramic content. Obviously, the whole experimental values are slightly lower than the theoretical ones. This phenomenon could be ascribed to the following two reasons: Firstly, the piezoelectric composites are more difficult to be electrically poled compared to the monolithic BNKT–ST ceramics. Secondly, slim and fragile ceramic rods are easy to crack during dicing. Both aspects lead to the lowering d_{33} value. As general, those values are reasonable and the trend is similar to that in predictions. By comparison, the experimental values of g_{33} match well with theoretical values. Particularly, the g_{33} value in low ceramic content range is much higher than high ceramic content, which is due to the great difference of ϵ_r [$g_{33} = d_{33}/(\epsilon_r \times \epsilon_0)$] with different ceramic content. For the application of biomedical ultrasonic transducers, d_{33} characterizes the ultrasonic beam transmission capability of a transducer, and its echo receiving sensitivity is related to g_{33} . One can even say that, g_{33} may be considered to be more important than d_{33} because a larger g_{33} can allow to detecting relatively feeble signals. This is of great

importance to the pulse-echo transducers because of the degradation of echo signal during propagations. The peak value of g_{33} is $91.5 \times 10^{-3} \text{ m}^2/\text{C}$, which is larger than the NKN-LT-LS fiber/epoxy 1–3 composite ($30 \times 10^{-3} \text{ m}^2/\text{C}$) [22] and NKLNT/epoxy 1–3 composite ($52.4 \times 10^{-3} \text{ m}^2/\text{C}$) [29]. In addition, the d_{33} value was found to show a slight increment when the ceramic volume fraction exceeds 0.3, however, the g_{33} value drastically drops beyond this ceramic content range. Therefore, a relatively low ceramic content should be favored because of a relatively large g_{33} value and a reasonable d_{33} value.

Another two important parameters of 1–3 composite for the application of ultrasonic transducers are the thickness coupling coefficient k_t and acoustic impedance Z . The coupling efficiency between the mechanical and electrical energies in the 1–3 composite is closely related to the thickness coupling coefficient k_t , which also determines the operating bandwidth of the transducers. The acoustic impedance Z demonstrates the acoustic transmission and reflection at the boundary because of different acoustic impedance values. The variation tendency of k_t and Z of the BNKT–ST ceramic/epoxy 1–3 composite with respect to the ceramic volume fraction ν is given in Fig. 5. The k_t value increases sharply in the low ceramic fraction range ($\nu < 0.2$) and keeps a constant value in the medium range ($0.2 < \nu < 0.8$). As $\nu > 0.8$, the k_t value decreases toward that of the bulk ceramic because of lateral clamping. As far as experimental values are concerned, 1–3 connectivity indeed effectively enhances the k_t value of composites, which is much higher than that of the bulk ceramic ($k_t \sim 0.487$). In other words, the k_t value of the 1–3 composite is approaching to the k_{33} value (~ 0.57) of monolithic BNKT–ST ceramic. Compared to the bulk ceramic, whose thickness extension or contraction is seriously restricted by its lateral clamping, ceramic rods in 1–3 composite could vibrate relatively freely due to weak clamping. That is to say, longitudinal vibration is not affected by lateral clamping for 1–3 composite, thus obtaining a higher k_t value. It is worth mentioning that the k_t value for the composite with $\nu = 0.57$ is slightly lower than the theoretical value, which could be attributed to influence of hybrid resonances, then k_t value ($k_t \sim 0.50$) of this 1–3 composite would be undermined, but still higher than that of monolithic ceramic ($k_t \sim 0.487$). In a word, the k_t value for the sample with $\nu = 0.276$ is 0.547, which is comparable to the BNKLBT-1.5 ceramic/epoxy composite ($k_t \sim 0.55$) [25] and is higher than the BSZT ceramics/epoxy composite ($k_t \sim 0.5$) [30]. For another parameter acoustic impedance Z , the experimental values increase monotonously with ν and match well with the theoretical prediction. As well known, bulk ceramic materials typically have higher acoustic impedance than the surrounding environment (for example, body tissues).

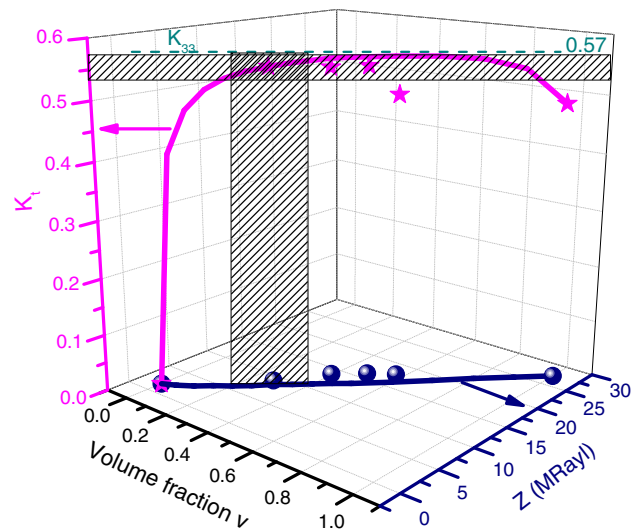


Fig. 5 Comparison between theoretical and experimental values of the thickness coupling coefficient and acoustic impedance of the BNKT–ST ceramic/epoxy 1–3 composite as a function of the ceramic volume fraction

The 1–3 composite, in which dense and stiff ceramic was replaced by a more compliant epoxy, distinctly decreased the Z value, especially in the low ceramic volume fraction. As a result, the energy transmission would be facilitated because of a good matching between the acoustic impedances of probe and body tissues.

According to the above discussions, the value of the thickness coupling coefficient k_t keeps almost constant in the medium range of ν (hatched section in the horizontal direction), however, acoustic impedance Z values increase linearly with the ceramic volume fraction in this range, and the k_t – Z relation is shown in Fig. 5. In the application of biomedical ultrasonic transducers as well as un-destructive evaluation, the k_t value was expected to be as high as possible, on the contrary, the Z value was expected to be as low as possible in a proper range, the value of k_t – Z should be compromised. As a matter of fact, it is not reasonable to optimize both k_t and Z simultaneously according to earlier reports [19, 31, 32]. Particularly, the acoustic impedance Z of 1–3 composite can be easily matched with a single quarterwave layer made from a common low impedance matching material [20, 33] and demonstrates that acoustic impedance is ideal at about 10 MRayls, which is also shown in the hatched section in the perpendicular direction in Fig. 5. Apparently, the ceramic volume fraction is in the vicinity of 0.3 and then both k_t and Z could reach a promising value simultaneously. Moreover, promising values of d_{33} and g_{33} can be also obtained in this ceramic volume range, as shown in Fig. 4. As to how to further lower the acoustic impedance Z using low impedance matching material to match with human body and water,

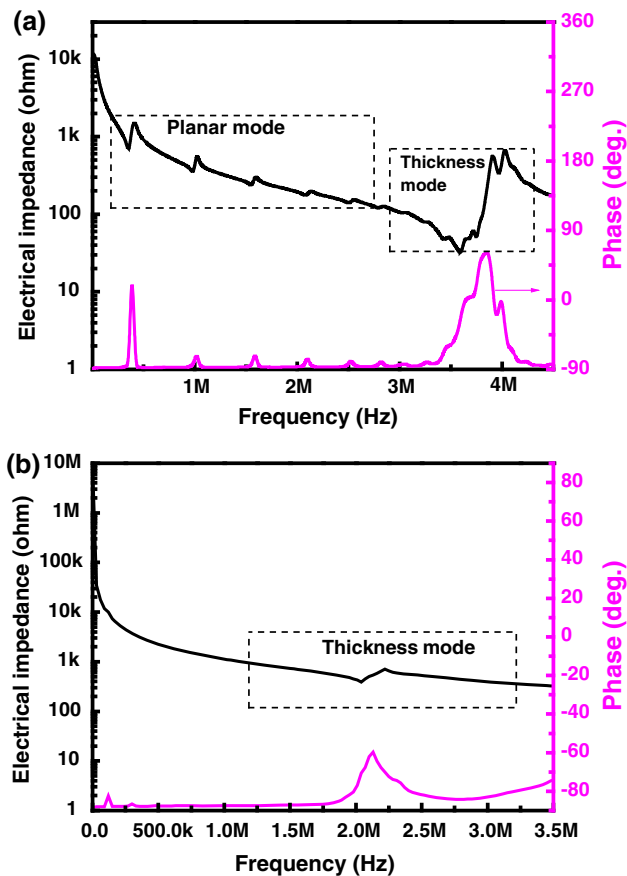


Fig. 6 Electrical impedance and phase versus frequency curves of **a** the monolithic BNKT–ST ceramics and **b** the 1–3 BNKT–ST ceramic/epoxy composites with $\nu = 0.276$

relevant work is in progress. Through the above analysis, the 1–3 composite with $\nu = 0.276$ may be a good candidate and was selected to investigate the resonance characteristics.

Figure 6 shows that the typical resonance characteristics of monolithic BNKT–ST ceramic and corresponding 1–3 composite with $\nu = 0.276$. As seen from Fig. 6a, two main resonance modes exist: planar and thickness modes, among which the planar mode is the typical working mode for bulk BNKT–ST ceramic. Regrettably, besides low resonance frequency, there are many hybrid resonance modes around main resonance modes, which is hazardous to the imaging due to the coupling among these resonance modes. By comparison, as shown in Fig. 6b, the thickness resonance mode become the main working mode for the 1–3 composite and its resonance frequency is more than 2 MHz without any undesirable hybrid resonance modes around the thickness resonance mode. That is to say, a clear single thickness mode with a relatively high resonance frequency was achieved. Therefore, the BNKT–ST ceramic/epoxy 1–3 composite can be expected to improve not only the

imaging quality but also the working frequency, which is of great importance to the application of biomedical ultrasonic imaging as well as nondestructive evaluation.

4 Conclusions

A modified dice-fill method was adopted to fabricate the BNKT–ST ceramic/epoxy 1–3 piezocomposites with different ceramic volume fractions from 0.2 to 0.6. The electromechanical properties of the BNKT–ST ceramic/epoxy 1–3 composite were characterized using the resonance method. The results indicated that the properties of the composite varied with the ceramic volume fraction and a relatively low ceramic volume fraction may be favored for the application of biomedical ultrasonic transducers. The 1–3 composites with $\nu = 0.276$ showed good electrical properties as follows: relatively high piezoelectric strain constant ($d_{33} \sim 104$ pC/N), enhanced piezoelectric voltage constant ($g_{33} \sim 91.5 \times 10^{-3}$ m²/C) and high electromechanical coupling coefficient ($k_t \sim 0.547$), moderate relative dielectric constant ($\epsilon_r \sim 128.4$) and relatively low acoustic impedance ($Z \sim 9$ Mrayls). Moreover, a single thickness mode can be obtained with a relatively high resonance frequency with more than 2 MHz. These promising results indicated that the present 1–3 lead-free piezocomposites would be suitable for the application of high frequency biomedical ultrasonic transducers as well as un-destructive evaluation.

Acknowledgments Financial support from the National Natural Science Foundation of China (Grant No. 51272060) is gratefully acknowledged.

References

1. B. Jaffe, W.R. Cook, H. Jaffe, *Piezoelectric Ceramics* (Academic Press, New York, 1971), pp. 135–171
2. G.H. Haertling, *J. Am. Ceram. Soc.* **82**(4), 797 (1999)
3. J. Rödel, W. Jo, K.T.P. Seifert, E.M. Anton, T. Granzow, *J. Am. Ceram. Soc.* **92**(6), 1153 (2009)
4. T.R. Shrout, S.J. Zhang, *J. Electroceram.* **19**, 111 (2007)
5. Y.H. Zhen, J.F. Li, *J. Appl. Phys.* **103**, 084119 (2008)
6. R. J. Meyer, J. P. Lopath, S. Yoshikawa, T. R. Shrout, *IEEE Ultrasonics Symposium* **2**, 915 (1997)
7. Y. Saito, H. Takao, T. Nonoyama, K. Takatori, T. Homma, T. Nagaya, M. Nakamura, *Nature* **432**, 84 (2004)
8. E. Cross, *Nature* **432**, 24 (2004)
9. G.A. Smolenskii, V.A. Isupov, A.I. Agranovskaya, N.N. Krainik, *Sov. Phys. Solid State (Engl. Transl.)* **2**(11), 2651 (1961)
10. C.F. Buhner, *J. Chem. Phys.* **36**, 798 (1962)
11. J. Suchanicz, K. Roleder, A. Kania, J. Handerek, *Ferroelectrics* **77**, 107 (1988)
12. Y.M. Li, W. Chen, J. Zhou, Q. Xu, H.J. Sun, R.X. Xu, *Mater. Sci. Eng. B* **112**, 5 (2004)
13. L.J. Liu, H.Q. Fan, S.M. Ke, X.L. Chen, *J. Alloy Compd.* **458**, 504 (2008)

14. C.H. Wang, *J. Ceram. Soc. Jpn.* **116**(5), 632 (2008)
15. N.M. Hagh, M. Allahverdi, A. Safari, *IEEE International Ultrasonics, Ferroelectrics and Frequency Control Joint 50th Anniversary Conference* (2004), pp. 246–249
16. R.E. Newham, D.P. Skinner, L.E. Cross, *Mater. Res. Bull.* **13**, 525 (1978)
17. D.P. Skinner, R.E. Newnham, L.E. Cross, *Mater. Res. Bull.* **13**, 599 (1978)
18. R.Y. Ting, *IEEE Trans. Ultrason. Ferroelectr. Freq. Control* **41**, 64 (1992)
19. A. Safari, V.F. Janas, A. Bandyopadhyay, *Ceram. Process.* **43**, 2849 (1997)
20. D. Zhou, K.H. Lam, Y. Chen, Q.H. Zhang, Y.C. Chiu, H.S. Luo, J.Y. Dai, H.L.W. Chan, *Sens. Actuat. A Phys.* **182**, 95 (2012)
21. K.H. Lam, M.S. Guo, D.M. Lin, K.W. Kwok, H.L.W. Chan, *J. Mater. Sci.* **43**, 1677 (2008)
22. B. Ma, R.Z. Zuo, J.Y. Yu, Y. Ran, Y. Wang, H.W.L. Chan, *J. Mater. Sci. Mater. Electron.* **22**, 1697 (2011)
23. K.C. Cheng, H.L.W. Chan, C.L. Choy, Q.R. Yin, H.S. Luo, Z.W. Yin, *IEEE Trans. Ultrason. Ferroelectr. Freq. Control* **50**, 1177 (2003)
24. Y.H. Zhen, J.F. Li, H.L. Zhang, *J. Electroceram.* **21**, 410 (2008)
25. S.H. Choy, W.K. Li, H.K. Li, K.H. Lam, H.L.W. Chan, *J. Appl. Phys.* **102**, 114111 (2007)
26. J. Yoo, J. Hong, H. Lee, Y. Jeong, B. Lee, H. Song, J. Kwon, *Sens. Actuat. A Phys.* **126**, 41 (2006)
27. H.L.W. Chan, J. Unsworth, *IEEE Trans. Ultrason. Ferroelectr. Freq. Control* **36**, 434 (1989)
28. F.F. Wang, C.J. He, Y.X. Tang, X.Y. Zhao, H.S. Luo, *Mater. Chem. Phys.* **105**, 273 (2007)
29. Z.Y. Shen, J.F. Li, R.M. Chen, Q.F. Zhou, K.K. Shung, *J. Am. Ceram. Soc.* **94**(5), 1346 (2011)
30. S.T.F. Lee, K.H. Lam, X.M. Zhang, H.L.W. Chan, *Adv. Mater. Res.* **254**, 90 (2011)
31. W.A. Smith, B.A. Auld, *Ferroelectrics* **38**(1), 40 (1991)
32. W. A. Smith, A. A. Shaulov, B. M. Singer, *Ultrasonics Symposium* 539 (1984)
33. W. Wang, S.W. Or, Q.W. Yue, Y.Y. Zhang, J. Jiao, B. Ren, D. Lin, C.M. Leung, X.Y. Zhao, H.S. Luo, *Sens. Actuat. A Phys.* **192**, 69 (2013)